Desalination and Water Treatment
www.deswater.com

39(2012)235–247
February

doi: 10/5004/dwt.2012.3359

Taylor & Francis
Taylor & Francis Group

Studies on arsenic adsorption by the use of aluminum anodizing sludge

Manassis G. Mitrakas*, Agamemnon K. Bakaloulis, Klontian T. Gkinis

Faculty of Chemical Engineering, Section of Chemistry, Aristotle University of Thessaloniki, 54124 Thessaloniki, Greece
Tel./Fax: +302310996248; email: manasis@eng.auth.gr

Received 17 November 2010; Accepted 1 March 2011

ABSTRACT

The objectives of this work were the testing of the suitability of **AL**uminum **A**nodizing **S**ludge (ALAS) as an arsenic adsorbent and the evaluation of the importance of its constituents on arsenic removal efficiency. The objectives were realized through leaching experiments and adsorption studies, both equilibrium and kinetic, using National Sanitation Foundation (NSF) water samples spiked with arsenic. The results showed that the major component of ALAS samples was that of gibbsite and major trace elements identified were chromium (300–2.8 × 10^3 mg/kg) and tin (250–1.9 × 10^3 mg/kg). ALAS samples were characterized as mesoporous materials with specific surface area varying between 60 and 216 m^2/g and judging by the low values of the physico-chemical parameters in their leachates, they are considered as non-hazardous materials. As(V) equilibrium adsorption data obeyed satisfactorily the Freundlich and Langmuir models with kinetics of adsorption governed by both surface adsorption and intraparticle diffusion. All ALAS samples were found to be inefficient adsorbents for As(III). In contrast, they were efficient adsorbents for As(V) with their adsorption capacity depending on gibbsite content with positive effect, phosphate content with negative effect and ambient pH, decreasing significantly as the pH value increased from 5 to 8. ALAS samples with a phosphate content up to 2.2% w/w were satisfactory As(V) adsorbents lowering an initial concentration of 100 μg/l well below the recommended limit for drinking water at a pH range of 5 to 8. In contrast, ALAS samples with higher phosphate content (5.1–8.1% w/w) failed to achieve this limit at pH values higher than 6.6. In conclusion, ALAS samples can be used not only as effective coagulants for wastewater treatment but at the same time as effective As(V) adsorbents provided that their phosphate content is not relatively high. ALAS with high phosphate content, however, comprise only a small part of the total ALAS produced because they originate from the production of shiny aluminum decoratives, which represent a small part of aluminum products.

Keywords: Aluminum anodizing sludge; Gibbsite; Physicochemical characteristics; Arsenic(V); Arsenic (III); Adsorption

1. Introduction

The knowledge that exposure to arsenic can provoke a variety of health problems to humans has led to extensive research on removing it from drinking water and wastewater. In connection to this WHO, USEPA, as well as the European Commission established a limit in drinking water of 10 μg/l arsenic. The limit for wastewaters disposal is somehow "flexible" depending on the sensitivity of the ecosystems they are discharged [1], with a lower limit for surface water intended for the abstraction of drinking water equal to 10 μg/l, while there are no defined limits for wastewater disposal to other surface water dischargers, since they are set by

*Corresponding author.

3rd International Conference on Small and Decentralized Water and Wastewater Treatment Plants (SWAT-III), Skiathos, Greece, 14–16 May 2010

the member states. Existing arsenic removal processes include; coagulation either with Al(III) or Fe(III) followed by filtration [2–7], whereas some researchers have examined the use of cationic or anionic polymers [5,8] to enhance removal, adsorption [9], zero valence iron [10], anion exchange [11], nano-filtration [12] and reverse osmosis [13]. Among these, adsorption seems to be a promising process, which in turn resulted in applying a great variety of solids for arsenic removal from water and wastewater [14] with ferric and aluminum oxy-hydroxides and activated alumina to be among the most effective adsorbents [15,16].

Aluminum anodizing is an electrochemical method of coating the surface of aluminum products with a thin layer of aluminum oxide (Al_2O_3). This process is a commonly used technique to provide the surface with high corrosion and abrasion resistance. Surface treatment of aluminum products – before anodizing – includes basic and acidic cleaning, that produces acidic wastewater rich in Al^{3+} that has to be disposed off in an acceptable manner. The wastewaters are neutralized either by NaOH or most frequently by $Ca(OH)_2$ and clarified. The supernatant is discharged to a sewer and the sludge is consolidated using a filter press. These solid wastes from the anodizing aluminum process are referred either as aluminum-rich sludge or more frequently as **AL**uminum **A**nodizing **S**ludge (ALAS) and the production in 2000 in EU countries was estimated to be about 10^5 metric tons per year [17]. ALAS is classified as a non hazardous material according to European Council Directive 33/2003 [18]. However, because of the great quantities of ALAS produced and its complex nature, its management presents difficulties with landfill disposal being currently a common practice. Complementary to this, ALAS has been reused in other industrial activities. The latter include ALAS addition in ceramic bodies [19–21], in the synthesis of pigments along with kaolin and various clays [22] and in the production of mullite–alumina refractory ceramics [23]. ALAS has also been tested in the treatment of municipal wastewaters and found that it can efficiently remove COD, suspended solids and microorganisms [24,25]. It has also been used successfully in the treatment of paint industry wastewater instead of the conventional inorganic coagulants [26]. From the above it becomes evident that ALAS has been proven an effective coagulant and since it consists mainly of aluminum hydroxide it seems reasonable to assume that it can also serve as an adsorbent for various organic and inorganic pollutants such as arsenic. Because of its expected and theoretically possible dual function, that is, as coagulant and adsorbent and furthermore because ALAS is a cost-free material in comparison to alternative coagulants such as commercial alum, it seems very attractive to study ALAS potential application on arsenic removal through a wastewater coagulation process. To the best of our knowledge, no study has appeared in the literature concerning the use of ALAS as arsenic adsorbent.

Therefore, the objectives of this work were the evaluation of ALAS as a potential adsorbent for As(III) and As(V) through equilibrium and kinetic studies and the investigation of the influence of its dominant physicochemical characteristics, such as aluminum, calcium, phosphate, carbonate and organic carbon, on specific surface area and isoelectric point (IEP) which eventually affect arsenic removal efficiency.

2. Materials and methods

2.1. ALAS samples selection and preparation

In order to investigate the chemical, physicochemical and mineralogical characteristics of ALAS, 14 samples from aluminum anodizing industry of Greece were collected in monthly intervals. Two samples were collected after modification of the production process of the industry to "chrome-free". The samples were homogenized and oven-dried at 105°C for 24 h. Then, they were stored over a silica gel in a desiccator for further chemical characterization, leaching tests and arsenic adsorption experiments. From the 14 samples, 5 of them were selected in order to evaluate arsenic species – As(V)/As(III) – adsorption and the influence of their physico-chemical and leaching characteristics on arsenic removal capacity. The five samples were so selected to represent a wide range in their major components, namely aluminum and phosphate, which are known to strongly affect arsenic adsorption [14]. The samples were consecutively numbered from 1 to 5 (Table 1). It is remarked that the presence of phosphate in certain

Table 1
Percentage of major components of ALAS samples used in arsenic adsorption experiments.

Parameter	Sample				
	1	2	3	4	5
	% Content				
Al	25.8	24.4	25.7	28.1	21.8
Ca	2.8	4.2	2.8	2.6	5.4
PO_4^{3-}	4.9	8.1	2.2	0.95	6.4
SO_4^{2-}	0.73	1.6	1.65	1.47	1.75
CO_3^{2-}	1.3	1.6	0.9	1.3	0.7
Organic carbon	1.44	1.95	1.73	1.9	1.9

ALAS samples originates from the process of production shiny mirror-type decoratives using an extra acidic treatment with phosphoric acid. However, the production capacity of shiny components generally comprises a small part of the total one and only a few industries have that option.

2.2. ALAS samples characterization

Dissolution. A 0.25 g dry sample was placed in a 100 ml PTFE beaker, 1 ml $HClO_4$, 20 ml HF were added and heated on a hot plate until white fumes of $HClO_4$ appeared. Then 20 ml of 6 N HCl were added and boiled for about 1 h until the residue had been completely dissolved. The solution was cooled and transferred to a 250 ml volumetric flask.

Metals. Metal concentration in ALAS samples and in their leachates, as well as arsenic concentrations in the adsorption experiments, were determined by atomic absorption spectrophotometry using a Perkin Elmer AAnalyst 800 instrument and either a flame or a graphite furnace.

Organic carbon (OC). The organic carbon of ALAS samples was determined using a ThermoFinnigan Flash EA 1112 CHNS Analyzer.

Sulfate and phosphate were determined according to the methods 4500-SO_4^{2-} D and 4500-P D, respectively, described in Standard Methods for Examination of Water and Wastewater (APHA, AWWA,WEF, 2005) [27].

Carbonate was determined in the solid samples by a volumetric-calcimeter method.

Mineralogical characterization. A TW1812 Phillips XRD equipment and a TG-DTA of TA INSTRUMENTS Model FDT2960 were used.

Particle size. A Microtrac – X100 particle size analyzer was used.

Surface area of the ALAS samples was estimated by nitrogen gas adsorption at liquid N_2 temperature using a micropore surface area analyzer.

Isoelectric point (IEP) of the ALAS particles was measured at room temperature (22 ± 2°C), using a Rank Brothers Micro-Electrophoresis Apparatus MkII.

2.3. Leaching

Leaching tests of ALAS samples were performed according to European Standard EN 12457-4 (2002) [28] using a solid to liquid ratio 1:10. Preliminary experiments showed that a solid to liquid ratio 1:2 resulted in a jelly mass with no liquid phase separation. Therefore a solid to liquid ratio 1:10 was chosen.

Metal concentration in the leachates was determined as described in Section 2.2.

Anions. Fluoride, chloride, nitrate, sulfate and phosphate concentration in the leachates were determined according to the methods 4500-F^-D, 4500-Cl^-F, 4500-NO_3^-C, 4500-SO_4^{2-}B and 4500-P D, respectively, described in Standard Methods for Examination of Water and Wastewater [27]. Cr(VI) concentration in the leachates was determined by the diphenylcarbazide method 350-Cr D [26] using a Lambda 2 UV/VIS spectrophotometer version 3.7 Perkin Elmer equipped with 10 cm path-length measurement cells, resulting in a detection limit of 1 μg/l.

Conductivity and pH in the leachates were measured according to the Standard Methods for Examination of Water and Wastewater [27].

Total Organic Carbon (TOC). A Shimadzu 500 TOC analyzer was used to measure TOC content of the leachates.

2.4. Reagents

Stock solutions of 1,000 mg/l were prepared for As(III) and As(V) from reagent grade $NaAsO_2$ and $Na_2HAsO_4 \cdot 7H_2O$, respectively, both dissolved in distilled water. Working standards were freshly prepared by proper dilution of the stock solution. NSF (National Sanitation Foundation) water samples were spiked either with As(III) or As(V) by adding the appropriate volume of working arsenic standard solution to achieve a 100 μg/l concentration. NSF water was prepared by dilution of the following reagents in 1 l of distilled water: 252 mg $NaHCO_3$, 12.14 mg $NaNO_3$, 0.178 mg $NaH_2PO_4 \cdot H_2O$, 2.21 mg NaF, 70.6 mg $NaSiO_3 \cdot 5H_2O$, 147 mg $CaCl_2 \cdot 2H_2O$ and 128.3 mg $MgSO_4 \cdot 7H_2O$.

2.5. Arsenic adsorption

Spiked NSF water samples were kept at room temperature (22 ± 2°C) for 24 h to achieve thermal equilibrium. Batch adsorption experiments were carried out at this temperature by placing the appropriate amount of ALAS, ranging between 25 and 500 mg/l, in a series of flask with 200 ml spiked water samples of initial arsenic concentration 100 μg/l either As(III) or As(V). The pH of spiked NSF water samples was adjusted at values of 5, 6.5, 7.5, 8 either by adding 0.1 N HCl or 0.1 N NaOH. The flasks were placed in an orbital shaker and equilibrium data for the adsorption isotherms were collected after 24 h shaking time since kinetic studies proved that at this time equilibrium had been reached. The adsorption kinetics data were collected from separate experiments at pH 7 for time intervals of 30, 60, 120, 240 min and 24 h. Samples were withdrawn after the predetermined time and filtered through a 0.45 μm pore size membrane filter. The filtrates were analyzed for residual arsenic concentration. In both kinetic and equilibrium experiments the amount of the arsenic adsorbed was calculated as the difference between the initial and the equilibrium arsenic concentration.

3. Results and discussion

3.1. Chemical and mineralogical characteristics of ALAS

A representative example of an X-ray diffractogram is presented in Fig. 1, which shows that the major component of ALAS samples were gibbsite (peaks at 2θ 18.4° and 20.5°) and $CaCO_3$ (peak at 2θ 29.2°). TG-DTA data (Fig. 2) showed a small shoulder at 230°C, which could be associated with the removal of strongly adsorbed water as well as the non-hydrogen-bonded surface hydroxyls and a strong endothermic peak at a temperature range 250 to 280°C due to the conversion of crystallized gibbsite to γ-Al_2O_3 [29]. The particle size of ALAS solids ranged between 1.635 and 88 μm, with the 50% of solids to be smaller than 10 μm and the 85% smaller than 50 μm (Fig. 3).

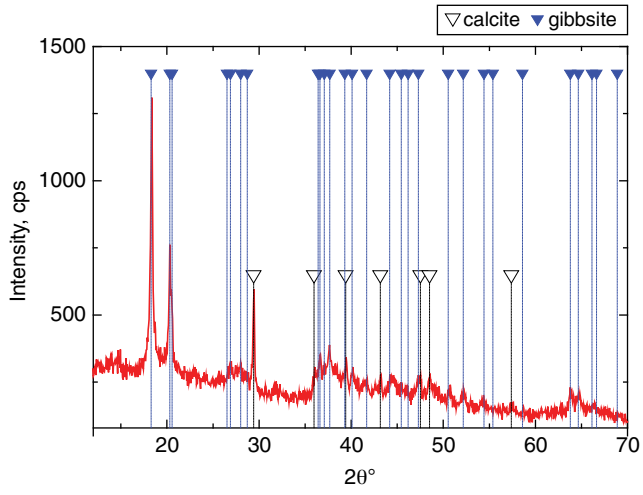

Fig. 1. X-ray diffractogram of sample No. 4. Main phases identified: gibbsite and $CaCO_3$.

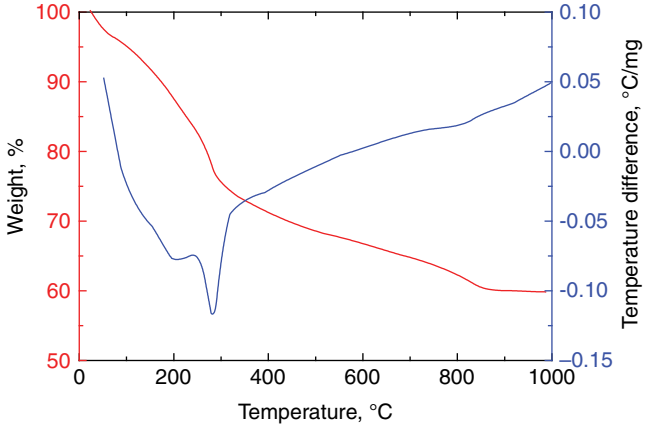

Fig. 2. TG-DTA curves of sample No. 4.

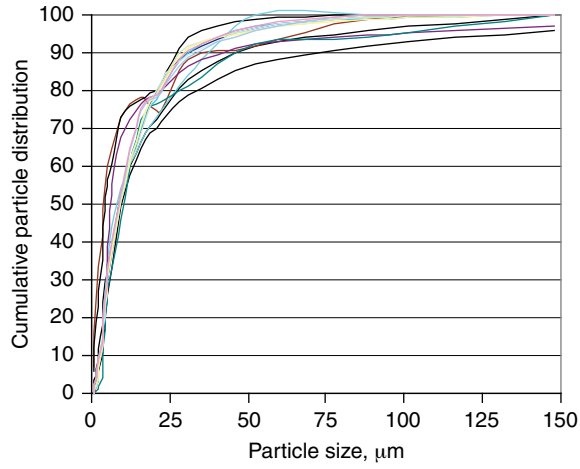

Fig. 3. Cumulative particle distribution of ALAS solids.

Aluminum content – on dry basis – in ALAS samples ranged between 17 and 28% w/w (Table 2), in agreement with the concentration determined by other investigators [17,21]. In addition, phosphate content ranged between 1 and 8.1% w/w, sulphate (2–5% w/w) and organic carbon (1.5–2% w/w). Other major components of ALAS were calcium (2.8–5.4% w/w) and carbonate (0.7–5.5% w/w), which were attributed to the practice of applying $Ca(OH)_2$ as a neutralizing agent at the wastewater treatment plant. The major trace elements concentrations determined were that of chromium (300–2.8 × 10^3 mg/kg) and tin (250–1.9 × 10^3 mg/kg) and were attributed to the surface treatment and coloring of the aluminum products in the anodizing process. However, chromium concentration in ALAS samples was significantly decreased between 100 and 150 mg/kg, when the "chrome-free" modification of the anodizing process was applied (Table 2).

3.2. Textural properties and porous structure of ALAS

According to the BDDT (Brunauer, Deming, Deming, Teller) classification, the nitrogen adsorption isotherms showed that ALAS samples were characterized as mesoporous materials (Fig. 4). The specific surface area of ALAS samples was calculated to be between 60 and 216 m^2/g (Table 3), which is common for aluminum oxyhydroxides, and in general favors their arsenic adsorption properties. Applying the Dubinin–Radushkevich equations on nitrogen adsorption isotherms of ALAS samples, the total pore volume was calculated along with the volume of micropores, the latter found to range between 13% and 27% of the total (Table 3).

Table 2
Physico-chemical characteristics of ALAS samples as well as of their leachates

Parameter	ALAS samples, mg/kg		Leachates, mg/kg		MAL[a]
	Range	Detection limit	Range	Detection limit	mg/kg
As	ND[b]	10	ND	0.05	2
Ba	ND	500	ND	0.1	100
Cd	1–5.3	0.01	ND	0.01	1
Cr	300–2.8 × 10^3	1	1.5–6.8	0.01	10
Cr[c]	100–150	1	02–0.4	0.01	10
Cu	47–225	20	ND	0.5	50
Fe	1.1 × 10^3–2.5 × 10^3	ND	1	–	
Mn	31–77	10	ND	0.5	–
Ni	10–42	10	ND	0.05	10
Pb	15–54	10	ND	0.05	10
Sb	ND	10	ND	0.1	0.7
Se	ND	10	ND	0.1	0.5
Sn	250–1.9 × 10^3	50	ND	5	–
Zn	73–976	10	0.3–1.1	0.2	50
Cl^-	–	–	240–1.45 × 10^3	50	15 × 10^3
F^-	–	–	8–16	0.1	150
SO_4^{2-}	2 × 10^4–5 × 10^4	–	12.5 × 10^3–18.5 × 10^3	100	20 × 10^3
Al	17 × 10^4–28 × 10^4	–	7–38	5	–
Ca	2.8 × 10^4–5.4 × 10^4	–	1 × 10^3–6.4 × 10^3	1	–
Mg	4.7 × 10^3–7.5 × 10^3	–	170–470	1	
K	100–940	–	31–63	1	–
Na	1.9 × 10^3–11 × 10^3	–	1.3 × 10^3–8.4 × 10^3	1	–
CO_3^{2-}	0.7 × 10^4–5.5 × 10^4	–	–	–	–
PO_4^{3-}	1 × 10^4–8 × 10^4	–	ND	0.1	–
OC[d]	1.5 × 10^4–2.0 × 10^4	–	TOC 335–1.4 × 10^3	2	50 × 10^3
pH			6.9–7.8	–	–
Conductivity, mS/cm			1.6–3.6	–	–

[a]Maximum acceptable limit for landfill disposal of non toxic wastes.
[b]Not detected.
[c]Chrome-free process.
[d]Organic carbon.

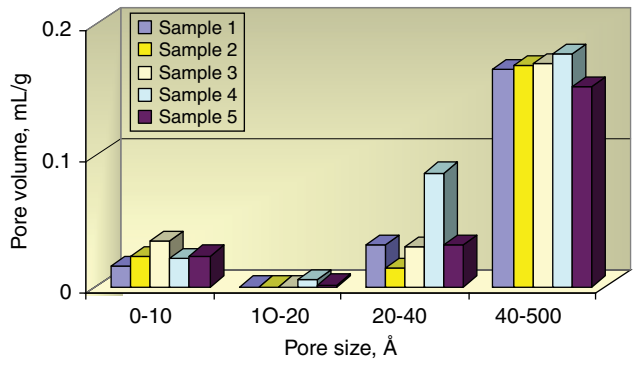

Fig. 4. Pore size distribution of ALAS samples.

Table 3
Textural properties of ALAS samples

Parameter	Sample				
	1	2	3	4	5
Surface area, m^2/g	92	60	115	216	94
Total pore volume cm^3/g	0.193	0.187	0.215	0.268	0.192
Micropore volume cm^3/g	0.025	0.028	0.053	0.072	0.042
Mean pore diameter Å	84	125	75	49	82

3.3. Estimation of IEP

Knowledge of IEP provides an important parameter for the explanation of the adsorption mechanism of an adsorbate at the metal oxy-hydroxide/water interface. Thus, by plotting ζ-potential as a function of the solution pH at constant ionic strength of 0.03 mol/l $NaNO_3$, the IEP of ALAS samples was determined as shown in Fig. 5. The relatively high IEP values of ALAS samples (8.4–12.5) calculated from the data of Fig. 5, can be attributed to the complex nature of the adsorbents and specifically to the combined effect of the following constituents:

- The presence of $CaCO_3$, which is generally associated with high IEP values [30]. The lower IEP value 8.4 of sample 5 may also be related to the lower CO_3^{2-} content (0.7%).
- The presence of Ca^{2+} which is specifically adsorbed moving the IEP to high values [31].

It must be stressed to the reader that these high IEP values of ALAS samples must not be confused with the IEP value of 8.3 of gibbsite [32]. Gibbsite as mentioned in Section 3.1 is the main component of ALAS samples and mainly responsible for arsenic adsorption. Therefore the subsequent discussion on the effect of pH on arsenic adsorption must be visualized and based on the value of IEP = 8.3 of pure gibbsite.

3.4. Characteristics of ALAS leachates

The ALAS leachates were characterized by the significantly low values of the most physicochemical parameters in comparison with the MAL for landfill disposal of non toxic wastes (Table 2) with the exception of sulphate concentration which was close enough to MAL for landfill disposal. Concerning chromium concentration in the leachates the following observations must be stressed:

- Almost three-quarters of chromium leached were in Cr(VI) form as shown by the slope of the regression curve of Fig. 6.
- The modification of the production process to "chrome-free" resulted in a one order lower concentration of chromium in the leachates (Table 2) and absence of Cr(VI).

Conclusively, all ALAS samples were classified as a non-hazardous waste [32] in agreement with the experimental results of other investigators [17,21]. In addition, the absence of Cr(VI) from ALAS samples produced from a "chrome-free" process favor their further use as coagulants.

3.5. Adsorption of arsenic

Arsenic occurs either as inorganic or organic complex compounds, in both its major trivalent or pentavalent states, depending on the prevailing redox conditions. Under typical pH conditions of a natural ecosystem (5–9) inorganic As(V) exists as an anion ($H_2AsO_4^-$/$HAsO_4^{2-}$), while As(III) is fully protonated and exists as an uncharged molecule (H_3AsO_3) [33]. Therefore, most treatment processes:

- Are more effective for the removal of ionic forms of As(V) in comparison to uncharged arsenite acid of As(III) and for this reason
- They involve an in situ oxidation of As(III) during treatment with zero-valent iron [10] or they embody a pre-oxidation step, either by a chemical reagent [34] or by bio-oxidation [35] for effective As(III) removal.

ALAS may be used as a coagulant in municipal wastewater treatment plants with high arsenic content

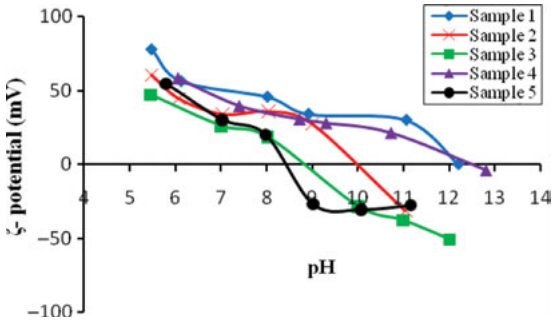

Fig. 5. Zeta potential of ALAS samples as a function of pH (0.03 M $NaNO_3$ background electrolyte).

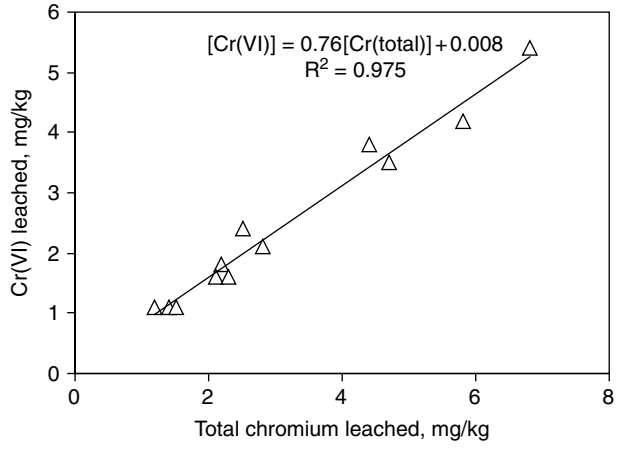

Fig. 6. Correlation between total chromium and Cr(VI) concentration in ALAS leachates.

and should be added before the biological sedimentation to increase the efficiency in solids separation as well as to decrease arsenic concentration in the effluent. The addition of ALAS at the end of the biological treatment step—and before sedimentation—where the biological oxidation of all arsenic forms to As(V) is ensured will increase arsenic removal efficiency. The initial arsenic concentration of 100 μg/l was selected as a reasonable compromise for studying ALAS samples efficiency, since the adsorption experiments were focused on their ability to reduce arsenic concentration down to the maximum contaminant limit (10 μg/l) of arsenic in potable water. This efficiency could serve as a criterion for water's aquifers protection. However, the arsenic concentration in water and in turn in wastewater varies significantly depending on the source of the water and its proximity to other arsenic spoils [15], but higher initial arsenic concentrations would simply require higher doses of ALAS. Apart from the municipal wastewater treatment ALAS can be also used in the treatment of metallurgical and mining wastewaters as coagulant to increase arsenic removal efficiency.

The selected ALAS samples differed in their aluminum content (gibbsite), with positive influence on arsenic adsorption and in phosphate with negative one. Therefore in the subsequent discussion any difference observed in arsenic adsorption between ALAS samples will be based on the difference on these two major components content.

3.5.1. Adsorption isotherms of As(V)

Arsenic (V) adsorption data were pretty well fitted to the Freundlich (Eq. 1):

$$q_e = K_F C_e^{1/n} \quad (1)$$

$$\frac{C_e}{q_e} = \frac{1}{K_L q_{max}} + \frac{C_e}{q_{max}} \quad (2)$$

as well as to the Langmuir (Eq. 2) equations and the parameters derived are summarized in Table 4. It is

Table 4
Isotherm (22 ± 2°C) parameters for arsenate adsorption onto ALAS samples

Sample	Equilibrium pH	Freundlich			Langmuir		
		K_F	$1/n$	R^2	q_{max} μg/mg	K_L l/μg	R^2
1	5.20	0.318	0.558	0.98	3.18	0.067	0.99
	6.45	0.109	0.632	0.93	1.63	0.044	0.97
	7.75	0.011	0.719	0.94	0.67	0.008	0.81
	8.10	0.003	0.803	0.95	0.43	0.003	0.95
2	5.15	0.271	0.593	0.98	3.35	0.052	0.99
	6.35	0.098	0.675	0.98	1.58	0.044	0.97
	7.65	0.024	0.648	0.93	0.72	0.014	0.88
	8.00	0.013	0.605	0.88	0.38	0.012	0.82
3	5.10	0.805	0.486	0.94	6.10	0.052	0.99
	6.60	0.100	0.651	0.99	1.86	0.034	0.98
	7.60	0.064	0.640	0.99	1.44	0.024	0.99
	8.05	0.091	0.472	0.96	0.85	0.045	0.95
4	5.25	1.153	0.343	0.97	5.91	0.067	0.96
	6.60	0.146	0.571	0.98	1.97	0.051	0.99
	7.60	0.104	0.553	0.99	0.94	0.069	0.99
	8.05	0.091	0.389	0.96	0.55	0.060	0.99
5	5.15	1.176	0.193	0.95	2.91	0.176	0.99
	6.50	0.063	0.621	0.95	1.28	0.025	0.94
	7.60	0.024	0.503	0.99	0.29	0.028	0.98
	8.00	0.013	0.472	0.90	0.12	0.075	0.89

noted that generally low values of R^2, for the Langmuir model, were observed at high pHs due to the low arsenic adsorption capacity of ALAS samples, resulting in a series of residual arsenic concentration very close to each other and thus sensitive to the precision of our measurements. Generally, q_e represents the amount of arsenic adsorbed (μg As/mg ALAS) at equilibrium arsenic concentration (C_e) and q_{max} the maximum adsorption capacity. K_F and $1/n$ are empirical fitting parameters of the Freundlich model representing the adsorption capacity and the intensity of the adsorption respectively, while the constant K_L (L μg^{-1}) of Langmuir's model is related to the affinity of the adsorbent for the adsorbate. The capacity of an adsorber for arsenate oxyanions removal is mainly a property determined by its surface morphology, charge and the ambient conditions such as pH and co-existing ions in water, with pH being considered as the determining factor. In addition, pH is interrelated to most of the other kind of interferences, since it influences speciation of ions, such as arsenate, phosphate and silicate.

By far the greatest influence on As(V) adsorption on amorphous metal oxides and oxy-hydroxides, such as ALAS is caused primarily by pH and secondarily by the forms and the charge of arsenate oxyanions. By increasing the pH, the fraction of the negatively charged surface groups increases, rendering the surface more negative and the repulsion of arsenate ions stronger, which eventually results in their less sorption. Lakshmanan et al., reported that, when using a total As(V) concentration of 0.67 μM (in the form of $H_2AsO_4^-$ and $HAsO_4^{2-}$), the concentration of $H_2AsO_4^-$ is significantly increased from 0.02 to 0.5 μM, when the pH drops from 8.5 to 6.5, resulting in a greater As(V) removal [3].

Among the co-existing ions in water, phosphate directly competes with arsenate for adsorption sites, since it has a strong affinity for adsorption onto metal oxides and oxy-hydroxides. In addition, as pH increases the portion of multivalent phosphate ions increases which in turn results in lower arsenate adsorption capacity. Silicate ions ($H_3SiO_4^-$) compete also with arsenic for adsorption sites and although they may have a weaker adsorption affinity than arsenate, silica is usually at a much higher concentration than arsenate and could play a major role in inhibiting arsenic removal. However, a typical silicic acid (H_4SiO_4) concentration of 20 mg Si/l in groundwater [9] ($pK_{a1} = 9.84$, $pK_{a2} = 13.2$), results in 9×10^{-3}, 0.116 mg and 1.107 mg Si/l as silicate ions ($H_3SiO_4^-$) at pH values 6.5, 7.5 and 8.5 respectively, which indicates the weak influence of silica on arsenic adsorption at pH values lower than 7.5 [3]. Inorganic ions such as sulfate, bicarbonate, chloride and nitrate generally have very little effect on adsorption [15].

It is obvious from the foregoing analysis that pH directly or indirectly is expected to be the major parameter affecting As(V) adsorption at pH range 5–8 studied in this paper. In addition, arsenic adsorption isotherms revealed that ALAS samples adsorption capacity for arsenic depended on its magnitude in their phosphate content. As a consequence the following discussion on arsenic adsorption is based on the effect of pH in conjunction with aluminum and phosphate content of ALAS samples.

Arsenic adsorption on ALAS samples (3 and 4) with low phosphate content, as a function of pH

The adsorption capacity (q_{max}) of ALAS samples 3 and 4 with low phosphate content (Table 1) was determined to be 6.1 and 5.91 μg As(V)/mg ALAS, respectively at pH 5.15 ± 0.1, which decreased by almost to one-third (1.86 and 1.97 μg As(V)/mg ALAS) at pH 6.5 ± 0.1 and drastically decreased by almost one order of magnitude (0.85–0.55 μg As(V)/mg ALAS) at pH 8 ± 0.1 (Table 4). These experimental data of Table 4 clearly show a significant decrease of the ALAS sample adsorption capacity with the increase of pH value.

The high influence of pH on ALAS adsorption capacity for As(V), resembles that of other aluminum compounds, such as activated alumina. Moreover, the determined q_{max} values are also similar to those reported for activated alumina. Tripathy and Raichur reported that an initial As(V) concentration of 10 mg/l was reduced to 40 μg/l by using 8 g/l alum- impregnated activated alumina(AIAA) at pH 7 resulting in an adsorption capacity of 1.24 μg As (V)/mg AIAA [16]. For example, this adsorption capacity lies between the values 1.56 and 0.7 μg As (V)/mg ALAS, calculated from adsorption data of sample 4 at C_e 40 μg/l and pH values 6.6 and 7.6, respectively, using the parameters of Table 4. Besides ALAS high As(V) adsorption capacity, adsorption isotherms revealed that ALAS samples with phosphate content lower than 2.2% w/w could efficiently reduce an initial concentration of 100 μg/l well below the recommended limit for drinking water at pH range 5–8 (Fig. 7, sample 3).

However, although ALAS samples with low phosphate content showed satisfactory arsenic adsorption capacity, similar to that of the commercially used activated alumina, their capacity were significantly lower in comparison to the corresponding $Al(OH)_3$, freshly precipitated in situ from alum [3,5]. The apparent reason for this higher arsenic loading on the in situ-formed $Al(OH)_3$ is that the As(V) ions form surface complexes on the short-chain oligomers/polymers $[Al_x(OH)_y^{z+}]$ of $Al(OH)_3$ floc particles with high surface area. Preformed gibbsite [$Al(OH)_3$] of ALAS simply does not have the available surface area in comparison to the freshly precipitated $Al(OH)_3$. As an example, the specific surface area of freshly precipitated gibbsite of 607 m^2/g was significantly reduced to 168 m^2/g after aging for one month [36].

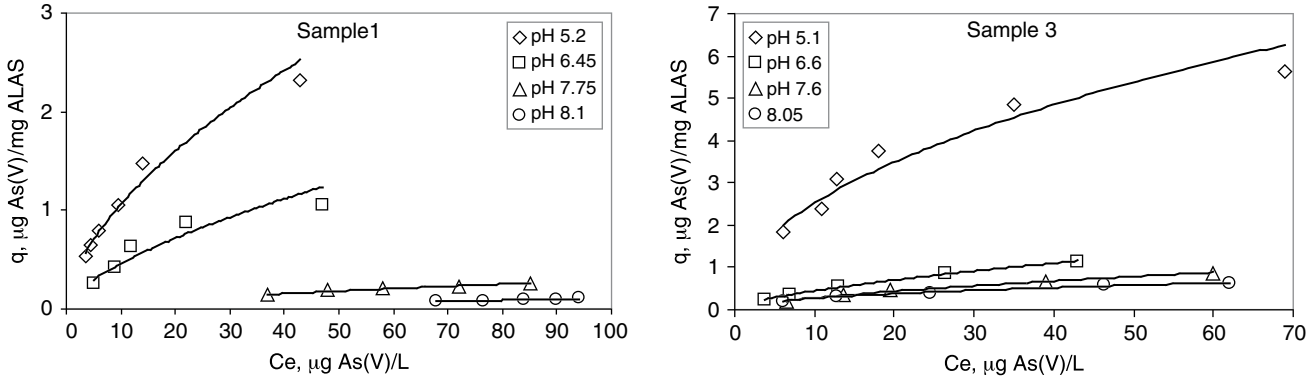

Fig. 7. Freundlich isotherms for As(V) adsorption of ALAS samples 1 and 3 as a function of pH.

Arsenic adsorption on ALAS samples (1,2,5) with high phosphate content

ALAS samples with high phosphate content (5.1–8.1% w/w) showed, at certain pH value, significantly lower As(V) adsorption capacity than that of samples with low phosphate content (Table 1). In addition, the As(V) adsorption was inhibited more strongly by pH increase. For example, although aluminum concentration of ALAS samples 1 and 3 was almost equal (Table 1), the As(V) adsorption capacity of sample 1 is almost half of that of sample 3 at high pH values probably due to inhibition of phosphate content. In addition ALAS samples with high phosphate content failed to achieve residual arsenic concentration close to the recommended limit for drinking water (Fig. 7, sample 1) at high pH values.

3.5.2. Adsorption kinetics of As(V) – intraparticle diffusion

The As(V) adsorption efficiency of ALAS was also examined at different time intervals. The time dependence curves of As(V) removal at pH 7 ± 0.1 is shown in Fig. 8. As(V) adsorption proceeded rapidly during the first 1 h, e.g. more than 80% of As(V) was adsorbed within 30 min and more than 95% within 1 h, after which it slowed down considerably, reaching the equilibrium at about 6 h. A similar behavior has been reported for activated alumina with As(V) adsorption proceeding rapidly during the first 1 h reaching equilibrium at about 6 h [16,37]. A fit to pseudo-second-order model of the As(V) kinetic adsorption data was observed (Table 5). The pseudo-second-order rate expression [16,37] is as follows:

$$t/q_t = 1/k_2 q_e^2 + t/q_e \quad (3)$$

where k_2 is the pseudo-second-order rate constant (mg μg^{-1} min^{-1}); q_t and q_e is the amount of As(V) adsorbed (μg As(V)/mg ALAS) at time t and at equilibrium, respectively. k_2 can be calculated from the slope and intercept of the plot t/q_t versus t. The high values of k_2 and R^2 (Table 5) suggest that the kinetics of adsorption obeyed a pseudo-second-order model in accordance to the adsorption of As(V) onto

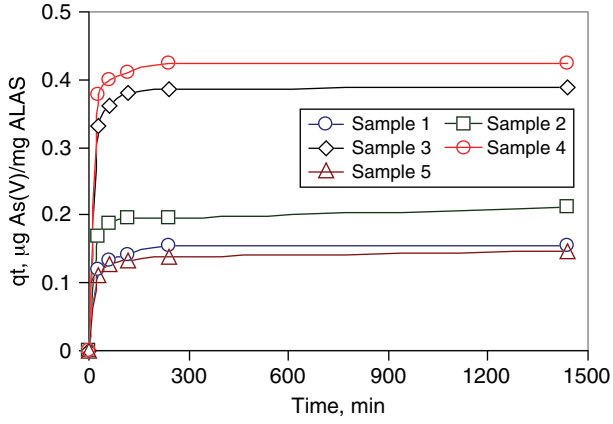

Fig. 8. Adsorption kinetic data of As(V) onto ALAS samples at pH 7 ± 0.1 (initial concentration 100 μg As(V)/l, adsorbent dose 0.5 g ALAS/l for samples 1,2,5 and 0.2 g ALAS/l for samples 3,4).

Table 5
Values of the rate constants k_2 (initial concentration 100 μg As(V)/l, adsorbent dose 0.5 g ALAS/l for samples 1,2,5 and 0.2 g ALAS/l for samples 3,4)

Sample	q_e (μg/mg)	Pseudo-second-order model	
		k_2 (mg μg^{-1}min^{-1})	R^2
1	0.16	0.538	0.999
2	0.23	0.339	0.999
3	0.39	0.629	1
4	0.42	0.768	1
5	0.15	0.366	0.999

activated alumina [16]. However, the estimated values of k_2 for ALAS samples (Table 5) were almost one order of magnitude higher than that reported for activated alumina [16,37]. These significantly higher adsorption rates of ALAS samples in comparison to activated alumina can be attributed to the fineness of the materials (Fig. 3).

Since ALAS samples are porous particles that are vigorously agitated during the adsorption period, it is logical to assume that the rate is not limited by mass transfer from the bulk liquid to particle external surface. One might then postulate that the rate limiting step may be film or intraparticle diffusion. Arsenate ions, however, are able to diffuse into the pore channel of mesoporous materials like ALAS, since their radius is small enough ($H_2AsO_4^-$:4.16 Å, $HAsO_4^{2-}$:3.97 Å) [37]. To verify this assumption the amount of As(V) adsorbed, q_t, at time t, was plotted according to the parabolic diffusion law, which is:

$$q_t = k_i t^{0.5} \quad (4)$$

where k_i is the diffusion rate constant (μg mg^{-1} min$^{-1/2}$), and the calculated values for ALAS samples presented in Table 6. The plot of q_t versus $t^{0.5}$ for ALAS sample 1 are shown in Fig. 9. The linear portion is attributed to the intraparticle diffusion effect and the plateau to the equilibrium. The linear part of all ALAS samples curves do not pass through the origin indicating that intraparticle diffusion is not the only rate controlling step for the adsorption of As(V) onto ALAS. k_i values were obtained from the slope of the linear portion of curves and presented in Table 6. These significantly lower diffusion rate constant values of ALAS samples in comparison to activated alumina [16,37] can also be attributed to the fineness of the materials (Fig. 3).

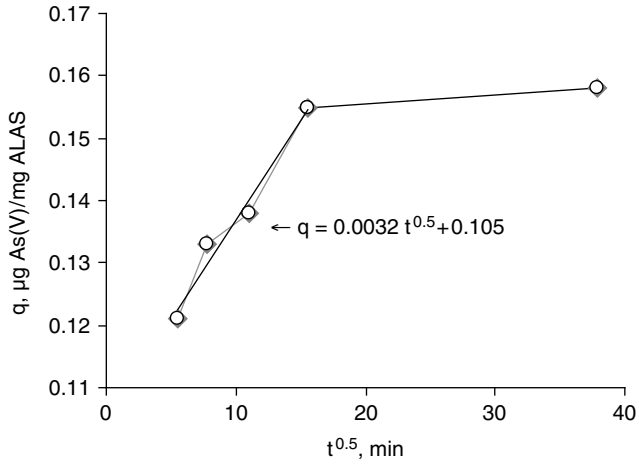

Fig. 9. Diffusion rate equation plots of arsenic adsorption on ALAS sample 1 (pH 7, initial concentration 100 μg As(V)/l, adsorbent dose 0.5 g ALAS/l).

3.5.3 Adsorption of As(III)

A significantly low As(III) adsorption efficiency was observed from all ALAS samples and as a consequence the adsorption experimental data failed to obey both the Freundlich and Langmuir models. For instance, by increasing the dose of ALAS samples from 50 to 500 mg/l at pH 6.5 ± 0.1 an initial As(III) concentration of 100 μg/l was marginally decreased to around 75 and 88 μg/l, by the low phosphate content samples (3,4) and high phosphate content samples (1,2,5), respectively (Fig. 10). A quantitative example can substantiate this low adsorption efficiency of ALAS for As(III) adsorption capacity in comparison to the As(V) one. Calculation of the adsorption capacity of sample 4 – with great efficiency – at equilibrium concentration 75 μg/l gave a value of q_{75} = 0.0125 μg As(III)/mg ALAS, which was more than two orders of magnitude lower than the corresponding q_{75} = 1.55 μg As(V)/mg ALAS, calculated by using the Freundlich isotherm constants of Table 4. As was the case with As(V) adsorption, pH showed strong influence on As(III) removal efficiency of ALAS sample (Fig. 11) due to:

- Existence of the non-ionic form H_3AsO_3 of As(III), which is the dominant species in the pH range of 5–8 and its adsorption onto ALAS surface is attributed only to weak Van der Waals forces.
- Co-occurring anions such as phosphate, which present a stronger affinity for the ALAS surface binding adsorption sites.

Such a low adsorption capacity of As(III) has also been reported both for activated alumina [38] and in situ freshly prepared $Al(OH)_3$. Indeed, Lakshmana et al.

Table 6
Values of intraparticle diffusion rate constant for ALAS samples (initial concentration 100 μg As(V)/l, adsorbent dose 0.5 g ALAS/l for samples 1,2,5 and 0.2 g ALAS/l for samples 3,4)

	Sample				
	1	2	3	4	5
k_i, μg mg^{-1} min$^{-1/2}$	0.0032	0.0023	0.0036	0.0029	0.0016

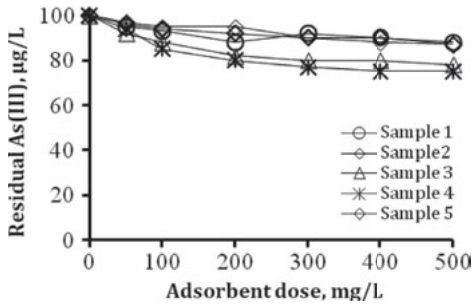

Fig. 10. Residual As(III) as a fuction of ALAS dose at pH 6.5 ± 0.1 (initial concentration 100 μg/l).

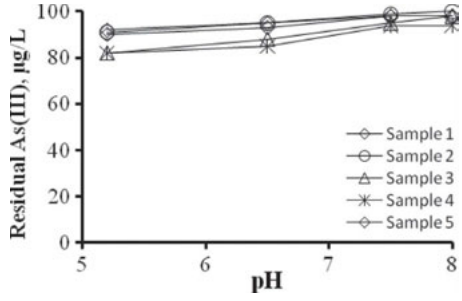

Fig. 11. Residual As(III) as function of pH (initial concentration 100 μg/l, adsorbent dose 100 mg/l).

failed to achieve residual As(III) concentration lower than 50 μg/l at pH 6.5 practicing coagulation with alum and finally concluded that "alum did not have any adsorption capacity for As(III)" [3].

3.5.4. Influence of physico-chemical characteristics of ALAS on As(V) adsorption

Simple Pearson's correlation coefficients (calculated by the statistical software SPPS, version 1.2) were used to assess the influence of the various physico-chemical characteristics of ALAS on arsenic adsorption. Generally, among the major ALAS components aluminum and phosphate were strongly related to the specific As(V) adsorption (q_{max}), as shown in Table 7, which in turn means that they strongly influence arsenic removal efficiency.

Specifically, aluminum which reflects gibbsite content of ALAS, showed a strong positive influence on the parameters related to arsenic removal such as q_{max} (r = 0.946), S_{sp} (r = 0.719), IEP (r = 0.789), as well as with the k_2 (r = 0.885). The weak positive correlation of q_{max} with IEP (r = 0.293) was to be expected since the measured IEP, as mentioned in Section 3.3, does not belong to true adsorbent (gibbsite) which is directly related with the q_{max}.

In contrast, phosphate was the key parameter with strong negative influence on the parameters related to arsenic removal such as q_{max} (r = −0.818), S_{sp} (r = −0.855) and k_2 (r = −0.967). The strong-positive relation of phosphate and sulfate with calcium and their strong-negative relation with arsenic adsorption and aluminum imply that these anions:

- Were primarily precipitated as calcium salts.
- Occupied adsorption sites of ALAS in priority during the neutralization–precipitation treatment of wastewater and their high concentration resulted in lower aluminum content. Also, the strong-negative relation of phosphate with the specific surface area of ALAS samples (Table 7, line 7, column 3) may illustrate the phosphate's interference on the aluminum hydroxide surface growth.

Table 7
Values of Pearson's correlation coefficients between the physicochemical characteristics of ALAS samples and As(V) adsorption at pH 6.5 ± 0.1

	q_{max}	S_{sp}	k_2	k_i	Al^{3+}	Ca^{2+}	PO_4^{3-}	SO_4^{2-}	CO_3^{2-}	OC[a]	IEP
q_{max}	1										
S_{sp}	0.694	1									
k_2	0.903	0.821	1								
k_i	0.608	−0.012	0.548	1							
Al^{3+}	0.946	0.719	0.885	0.589	1						
Ca^{2+}	−0.906	−0.531	−0.885	−0.829	−0.931	1					
PO_4^{3-}	−0.818	−0.855	−0.967	−0.395	−0.753	0.748	1				
SO_4^{2-}	−0.235	−0.076	−0.300	−0.548	−0.498	0.568	0.091	1			
CO_3^{2-}	0.330	−0.042	0.015	0.284	0.477	0.351	0.213	−0.529	1		
OC	−0.097	0.161	−0.280	−0.733	−0.220	0.503	0.164	0.755	0.006	1	
IEP	0.293	0.540	0.565	0.156	0.789	−0.680	−0.384	−0.835	0.622	−0.364	1

[a]Organic carbon.

Calcium content was negatively related to As(V) removal (q_{max}), either because its increase resulted in aluminum content decrease, as it was also previously mentioned for phosphate and sulfate, or most probably because calcium existed as phosphate salt, which phosphate strongly interfere arsenic adsorption. Organic carbon, sulfate, as well carbonate, showed no significant relation with the parameters affecting arsenic removal.

4. Conclusions

ALAS samples consist mainly of aluminum hydroxide (gibbsite) and are characterized as a non hazardous, inert material. They can be used, not only as effective coagulants for wastewater treatment but at the same time as potential As(V) adsorbents. The results of this study showed that As(V) adsorption obeyed satisfactorily the Freundlich and Langmuir models with kinetics of adsorption governed by both surface adsorption and intraparticle diffusion being fast enough reaching a practical equilibrium in 1 h. The major components of ALAS samples affecting arsenic adsorption were aluminum (gibbsite) and phosphate content. Aluminum content had a positive effect on As(V) adsorption whereas phosphate a negative one. All ALAS samples were found to be inadequate adsorbents towards As(III). The As(V) as well as As(III) adsorption capacity of ALAS was significantly decreased as the pH value was gradually increased from 5 to 8. ALAS samples with a phosphate content up to 2.2% w/w were satisfactory As(V) adsorbents lowering an As(V) initial concentration of 100 μg/l well below the recommended limit for drinking water at pH range 5–8. In contrast, ALAS samples with high phosphate content (5.1–8.1% w/w) failed to achieve residual As(V) concentration close to the recommended limit for drinking water at pH values higher than 6.6. Finally, since ALAS samples with high phosphate content are very rare worldwide, the majority of them should be considered as effective arsenate adsorbents.

Acknowledgements

The comments and suggestions of the two anonymous referees are gratefully acknowledged.

References

[1] European Council Directive 60/23-10-2000, establishing a framework for Community action in the field of water policy.
[2] M. Mitrakas, P. Panteliadis, V. Keramidas, R. Tzimou-Tsitouridou and C. Sikalidis, Predicting Fe^{3+} dose for As(V) removal at pHs and temperatures commonly encountered in natural waters, Chem. Eng. J., 155 (2009) 716–721.
[3] D. Lakshmanan, D. Clifford and G. Samanta, Arsenic removal by coagulation with aluminum, iron, titanium and zirconium. J. Am. Water Works Assoc., 100(2) (2008) 76–88.
[4] J.D. Chwirka, C. Colvin, J.D. Gomez and P.A. Mueller, Arsenic removal from drinking water using the coagulation/microfiltration Process, J. Am. Water Works Assoc., 96 (2004) 106–115.
[5] A.I. Zouboulis, I.A. Katsoyiannis, Removal of arsenates from contaminated water by coagulation – direct filtration, Separ. Sci. Technol., 37 (2002) 2859–2873.
[6] J.G. Hering, P-Y. Chen, J.A. Wilkie, M. Elimelech and S. Liang, Arsenic removal by ferric chloride, J. Am. Water Works Assoc., 88 (1996) 155–167.
[7] R.C. Cheng, S. Liang, H-C. Wang and M.D. Beuhler, Enhanced coagulation for arsenic removal, J. Am. Water Works Assoc., 86 (1994) 79–90.
[8] M. Edwards, Chemistry of arsenic removal during coagulation and Fe-Mn oxidation, J. Am. Water Works Assoc., 86 (1994) 64–78.
[9] G. Amy, H. Chen, A. Drizo, U. von Gunten, P. Brandhuber, R. Hund, Z. Chowdhury, S. Kommineni, S. Sinha, M. Jekel and K. Banerjee, Adsorbent treatment technologies for arsenic removal, Am. Water Works Assoc. Research Foundation Report, 2005.
[10] O.X. Leupin and S.J. Hug, Oxidation and removal of As(III) from aerated groundwater by filtration through sand and zero-valent iron, Water Res., 39 (2005) 1729–1740.
[11] G.L. Ghurye, D.A. Clifford, A.R. Tripp, Combined arsenic and nitrate removal by ion exchange, J. Am. Water Works Assoc., 91 (1999) 85–96.
[12] Y Sato, M. Kang, T. Kamei and Y. Magara, Performance of nanofiltration for arsenic removal, Water Res., 36 (2002) 3371–3377.
[13] M. Kang, M. Kawasaki, S. Tamada, T. Kamei and Y. Magara, Effect of pH on the removal of arsenic and antimony using reverse osmosis membranes, Desalination, 131 (2002) 293–298.
[14] D. Mohan and C.U. Pittman Jr., Arsenic removal from water/wastewater using adsorbents – A critical review, J. Hazard. Mater., 142 (2007) 1–53.
[15] K. Henke, Environmental Chemistry, Health Threats and Waste Treatment, John Wiley & Sons, West Sussex, United Kingdom, 2009.
[16] S.S. Tripathy and A.M. Raichur, Enhanced adsorption of activated alumina by impregnation with alum for removal of As(V) from Water, Chem. Eng. J., 138 (2008) 179–186.
[17] A.M. Seabra, D.A Pereira, C.M. Boia and J.A. Labrincha, Pretreatment needs for recycling of Al-rich anodizing sludge as a ceramic raw material. In: C.S. Gomes (Ed.), Proceedings of the 1st Latin American Clay Conference, Funchal, Portugal, 2 (2000) 176–181.
[18] European Council Directive 33/16-01-2003, Council Decision of 19 December 2002 establishing criteria and procedures for the acceptance of waste at landfills pursuant to Article 16 and Annex II to Directive 1999/31/EC.
[19] M. J. Ribeiro, D.U. Tulyaganov, J.M. Ferreira and J.A. Labrincha, Production of Al – rich sludge – containing ceramic bodies by different shaping techniques, J. Mat. Proc. Technol., 148 (2004) 139–146.
[20] A.P. Novaes de Oliveira, V. Gomes, D. Hotza, O.R.K. Montedo, R. Piccoli and F.R. Perei, Aluminum rich sludge as raw material for the ceramic industry, Interceram., 52(1) (2003) 44–46.
[21] J. Ribeiro, D.U. Tulyaganov, J.M. Ferreira and J.A. Labrincha, Recycling of Al-rich industrial sludge in different ceramic bodies, Ceram. In., 28(3) (2002) 319–326.
[22] V. Gomes, J.A. Labrincha and A.P. Novaes de Oliveira, Synthesis of pigments using Al-rich sludge, Am. Ceram. Soc. Bull., 5 (2005) 9501–9503.
[23] D.U. Tulyaganov, S.M.H. Olhero, M.J. Ribeiro, J.M. Ferreira and J.A. Labrincha, Mullite – alumina refractory ceramics obtained from mixtures of natural common materials and recycled Al-rich anodizing sludge, J. Mat. Synt. Proc., 10(6) (2002) 311–318.
[24] A. Correira, T. Chambino, L. Goncalves, A. Franco, R. Goncalves, A. Goncalves, V. Limpo, F. Delmas, C. Nogueira and F.Bartolomeu, Municipal wastewater treatment with anodizing solid waste, Desalination, 185 (2005) 341–350.

[25] T. Chambino, A. Correira, A. Goncalves and F. Bartolomeu, Reuse of industrial waste sludge, Wastewater Treatment International Water Association (IWA) 2nd World Water Congress. Proceedings in CD-Rom, Berlin, 2001.
[26] A. Correira, T. Chambino, L. Goncalves, C. Ribeiro and F. Bartolomeu, Use of solid waste from surface treatment of aluminum as coagulant, 7th Conference on Environmental Science and Technology, Ermoupolis, Greece, University of the Aegean, T. D. Lekkas eds, 129–138, 2001.
[27] "Standard Methods for the examination of water and wastewater". Apha AWWA WEF, 18th edition, 1992.
[28] European Standard EN 12457-4, 2002. Characterisation of waste – Leaching – Compliance test for leaching of granular waste materials and sludge – Part 1: One stage batch test at a liquid to solid ratio of 10L/kg for materials with high solid content and with particle size below 10 mm (without or with size reduction).
[29] S. Shen, P.S Chow and F. Chen, Synthesis of submicron gibbsite platelets by organic – free hydrothermal crystallization process, J. Crystal Growth, 292 (2006) 136–142.
[30] E. Chibowski, L. Hotysz and A. Szczes, Time dependent changes in zeta potential of freshly precipitated calcium carbonate, Colloids Surf. A. Physicochem. Eng. Aspects, 222 (2003) 41–54.
[31] R.M. Cornell and U. Schwertmann, The iron oxides: Structure, properties, reactions, occurrence and uses, VCH, Weinheim, 2003.
[32] M. Kosmulski, The pH-dependence surface charging and the points of zero charge, J. Colloid Interf. Sci., 253 (2002) 77–87.
[33] W.D. Schecher and D.C. McAvoy, MINEQL$^+$, v. 3.0, User's Manual, Hallowell, Maine, USA,1999.
[34] G. Ghurye and D. Clifford, As(III) oxidation using chemical and solid-phase oxidants, J. Am. Water Works Assoc., 96 (2004) 84–96.
[35] Katsoyiannis I.A. and A.I. Zouboulis, Application of biological processes for the removal of arsenic from groundwaters, Water Res., 38 (2004) 17–26.
[36] K.C. Makris, W.G. Harris, G.A. O'Connor and H. El-Shall, Long-term phosphorus effects on evolving physicochemical properties of iron and aluminum hydroxides, J. Colloid Interf. Sci., 287 (2005) 552–560.
[37] Y. Kim, Ch. Kim, I. Choi, S. Rengaraj and J. Yi, Arsenic removal using mesoporous alumina prepared via a templating method, Environ. Sci. Technol., 38 (2004) 924–931.
[38] T.S. Singh and K.K. Pant, Equilibrium, kinetics and thermodynamic studies for adsorption of As(III) on activated alumina, Separ. Pur. Technol., 36 (2004) 139–147.